Adaptive Machine Learning-based Real-time 3D Inversion for Coherent Diffraction Imaging

LA-UR-21-29504

Alexander Scheinker (AOT-AE), Reeju Pokharel (MST-8)

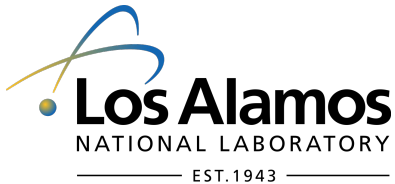

Bragg coherent diffractive imaging enables us to view the atomic disorder and defects within a single crystal

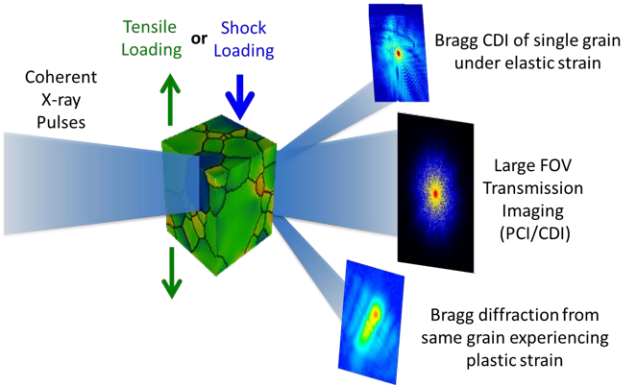

Sayre, Acta Cryst 5, 843 (1952)
Miao et al., Nature 400, 342 (1999)
Miao and Sayre, Act Cryst A56, 596 (2000)

- **BCDI employs coherent beam to image incoherent domains in a crystal with atomic resolution**

$$\rightarrow(\mathbf{r}) = s(\mathbf{r})e^{-i\phi(\mathbf{r})}$$

$$I(\mathbf{w}) = \left| \iiint \rightarrow(\mathbf{r})e^{i\mathbf{w}\cdot\mathbf{r}}d\mathbf{r} \right|^2$$

Machine Learning and Adaptive Feedback

Neural Networks

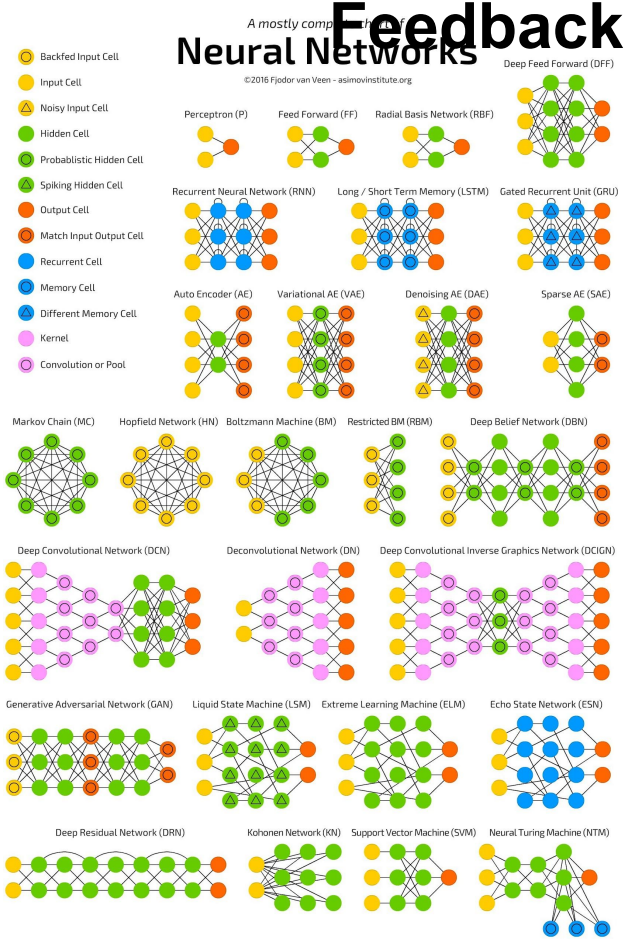

Surrogate models Big data

Adpative Feedback

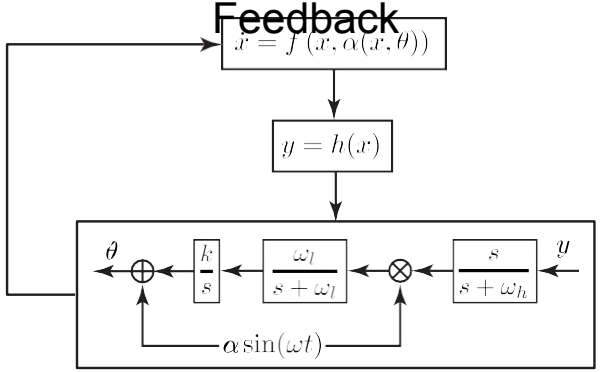

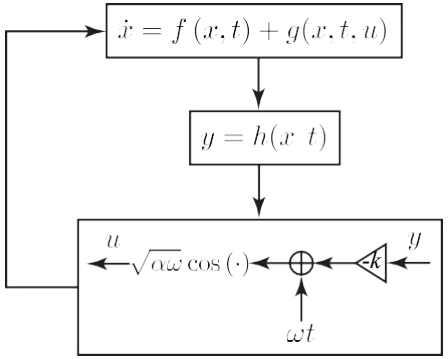

Real time

3D Convolutional Neural Networks for BCDI

Institute of Materials Science Rapid Response project (No. RR2020-R&D-1)

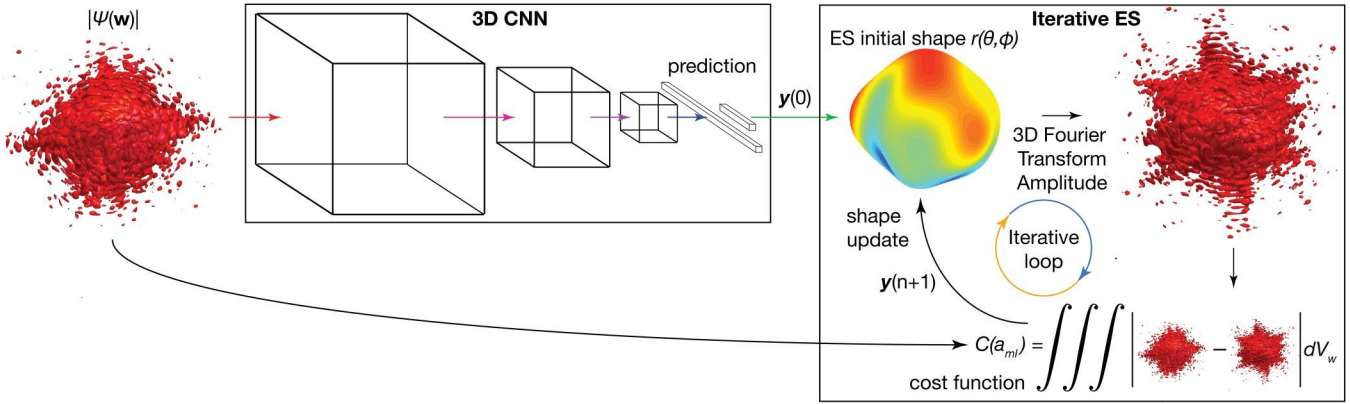

A. Scheinker and R. Pokharel. "Adaptive 3D convolutional neural network-based reconstruction method for 3D coherent diffraction imaging." *Journal of Applied Physics* 128.18 (2020): 184901.

Bounding surface

$$\hat{s}(\theta,\phi) = \sum_{l=0}^{N} \sum_{m=-l}^{l} \hat{a}_{ml} Y_l^m(\theta,\phi),$$

Electron density

$$\hat{\rho}(\mathbf{r},\theta,\phi) = \begin{cases} d, & |\mathbf{r}| \le \hat{s}(\theta,\phi) \\ 0, & |\mathbf{r}| \ge \hat{s}(\theta,\phi) \end{cases}$$

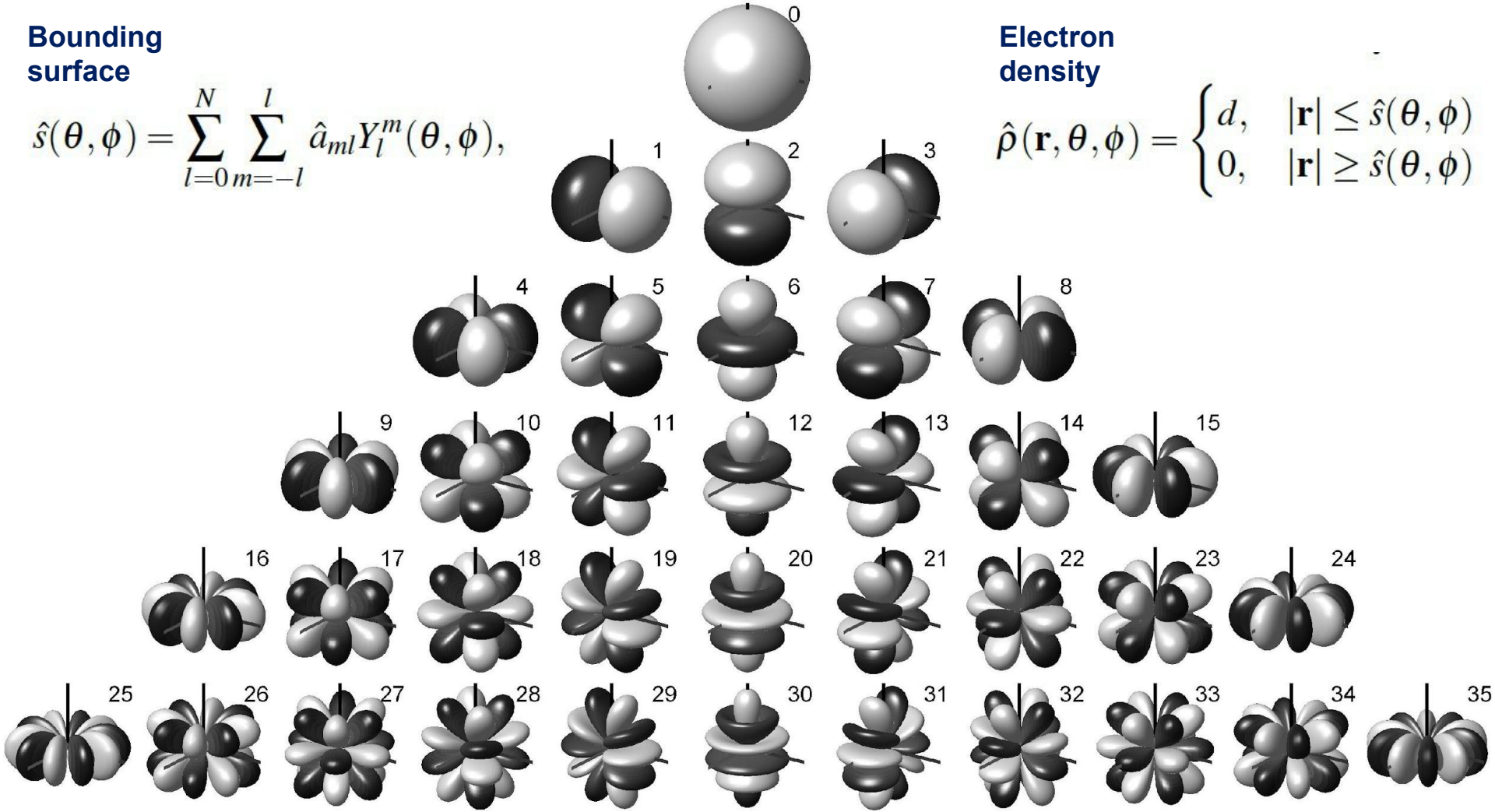

reeju@lanl.gov

Non-uniform 3D Structures

Measured intensity

$$I(\mathbf{w}) = \iint \rho(\mathbf{r}_1)\rho^{\star}(\mathbf{r}_2)\exp\left[i\mathbf{q}\left(\mathbf{r}_1-\mathbf{r}_2\right)\right]d\mathbf{r}_1 d\mathbf{r}_2$$
$$= \psi(\mathbf{w})\psi^{\star}(\mathbf{w})$$
$$= |\psi(\mathbf{w})|^2 \exp\left[i\phi(\mathbf{w})\right]\exp\left[-i\phi(\mathbf{w})\right]$$
$$= |\psi(\mathbf{w})|^2,$$

Bounding surface

$$\hat{s}(\theta,\phi) = \sum_{l=0}^{N}\sum_{m=-l}^{l} \hat{a}_{ml} Y_l^m(\theta,\phi),$$

Non-Uniform Interior using radial basis function (RBF) expansion

$$\rightarrow(\mathbf{r}, \checkmark, ¢) = \begin{cases} d(\mathbf{r}), & |\mathbf{r}| \square\ s(\checkmark, ¢) \\ 0, & |\mathbf{r}| \blacklozenge s(\checkmark, ¢) \end{cases}, \qquad d(\mathbf{r}) = \sum_{i=1}^{N_R} a_i e^{-\text{✏}_i \|\mathbf{r}-\mathbf{r}_i\|^2}$$

A. Scheinker and R. Pokharel. "Adaptive 3D convolutional neural network-based reconstruction method for 3D coherent diffraction imaging." *Journal of Applied Physics* 128.18 (2020): 184901.

Adaptive Tuning for 3D Shapes

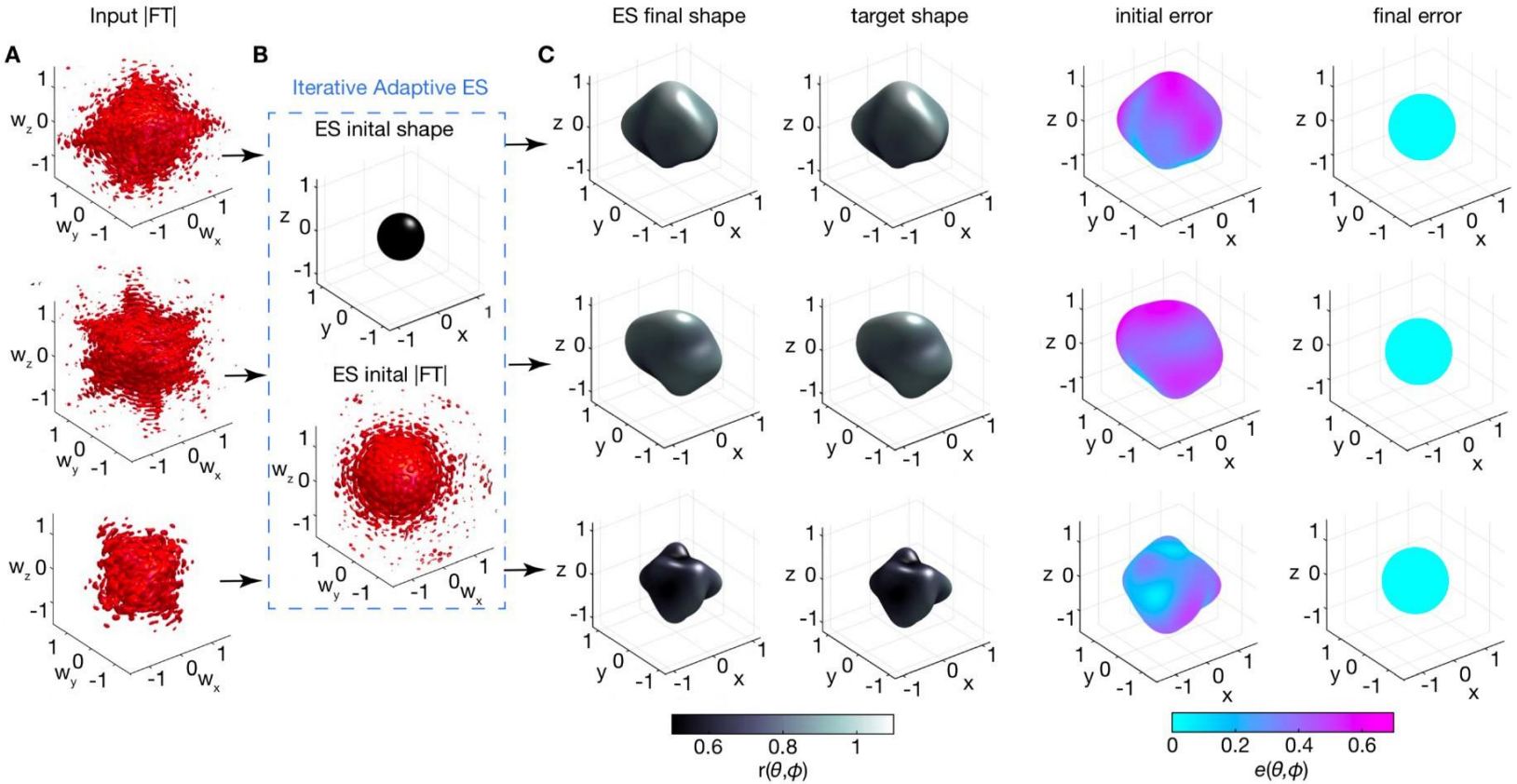

A. Scheinker and R. Pokharel. "Adaptive 3D convolutional neural network-based reconstruction method for 3D coherent diffraction imaging." *Journal of Applied Physics* 128.18 (2020): 184901.

Non-uniform 3D Structures

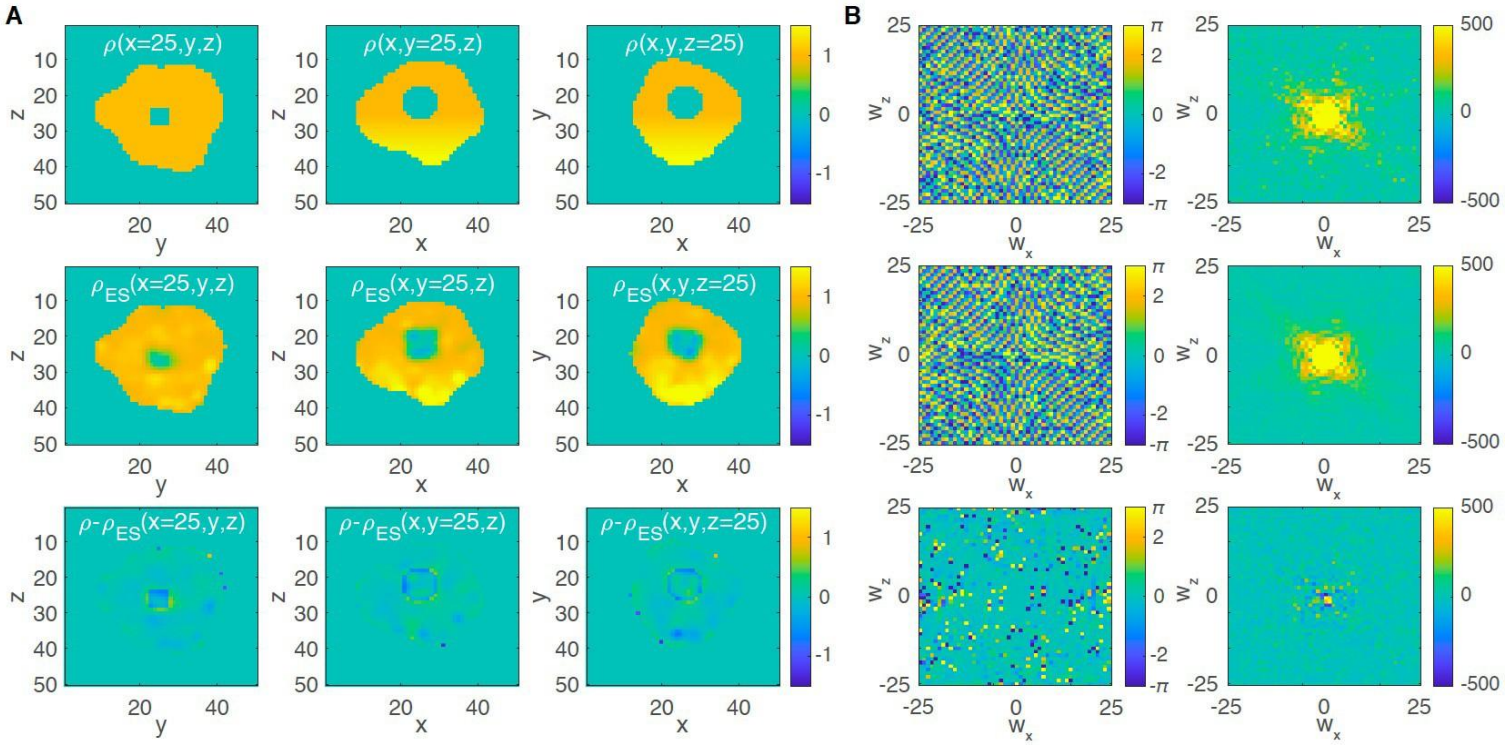

A. Scheinker and R. Pokharel. "Adaptive 3D convolutional neural network-based reconstruction method for 3D coherent diffraction imaging." *Journal of Applied Physics* 128.18 (2020): 184901.

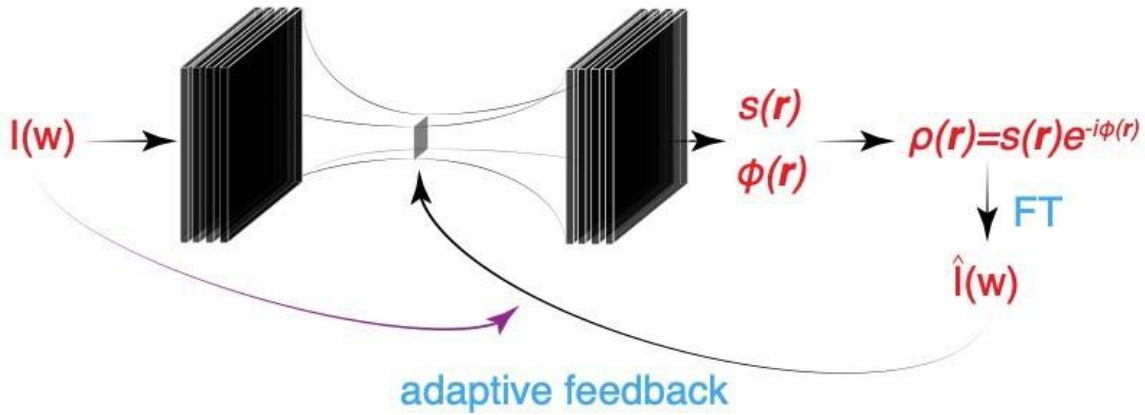

$$I^{1}_{i_1,j_1} = b^{1} + \sum_{n=1}^{N_f} w_n \rightarrow f_n \left(b^{0}_{n} + \sum_{i=-1}^{1} \sum_{j=-1}^{1} F_{0,ij,n} \rightarrow I^{0}_{i_0+i,j_0+j} \right)$$

Low-Dimension Latent Space Projections

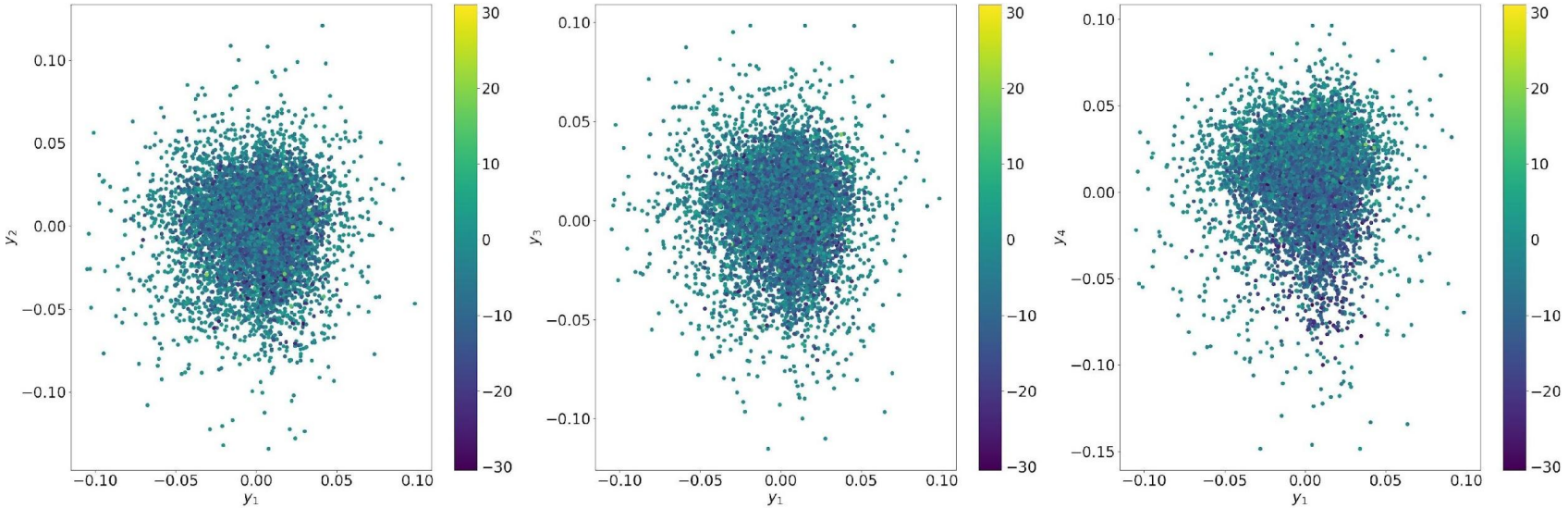

Low-Dimension Latent Space Projections

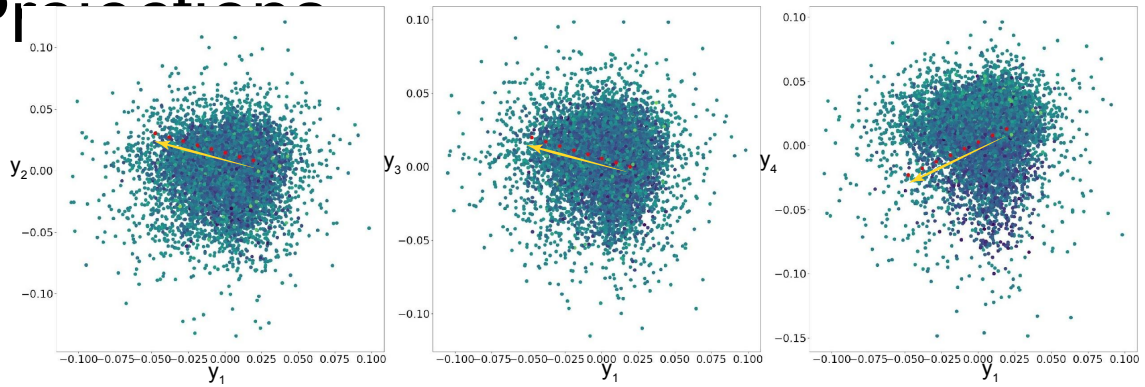

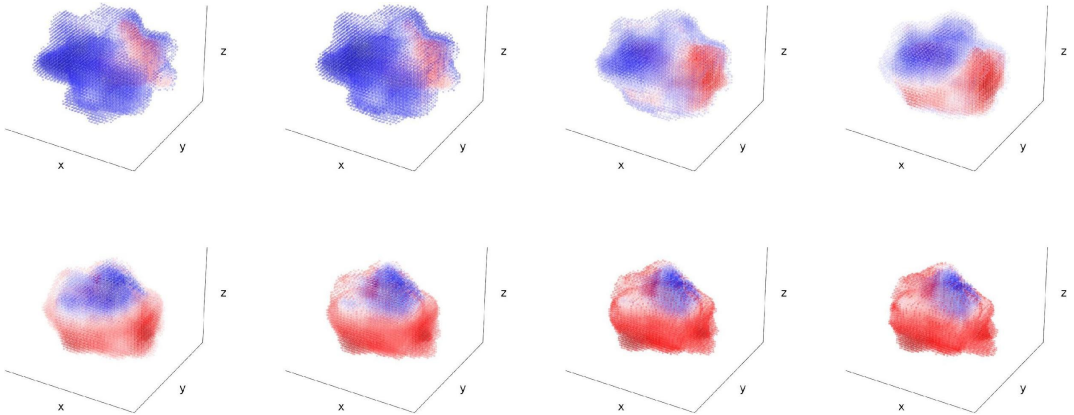

Low-Dimension Latent Space Projections

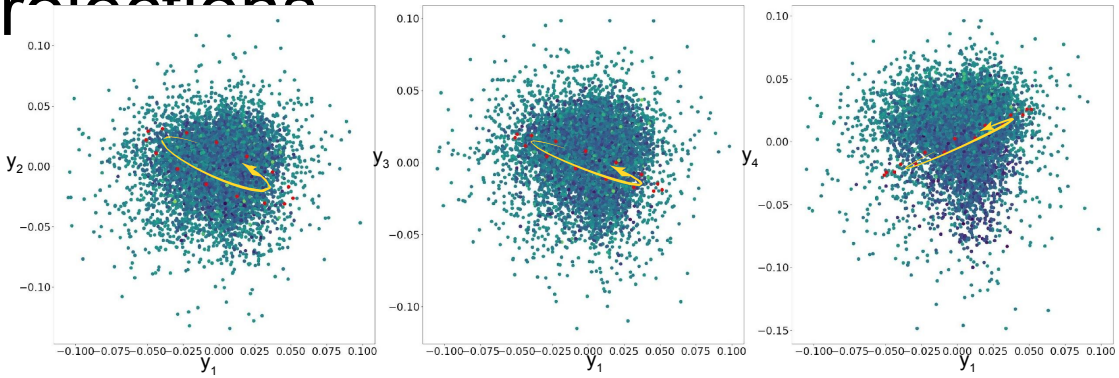

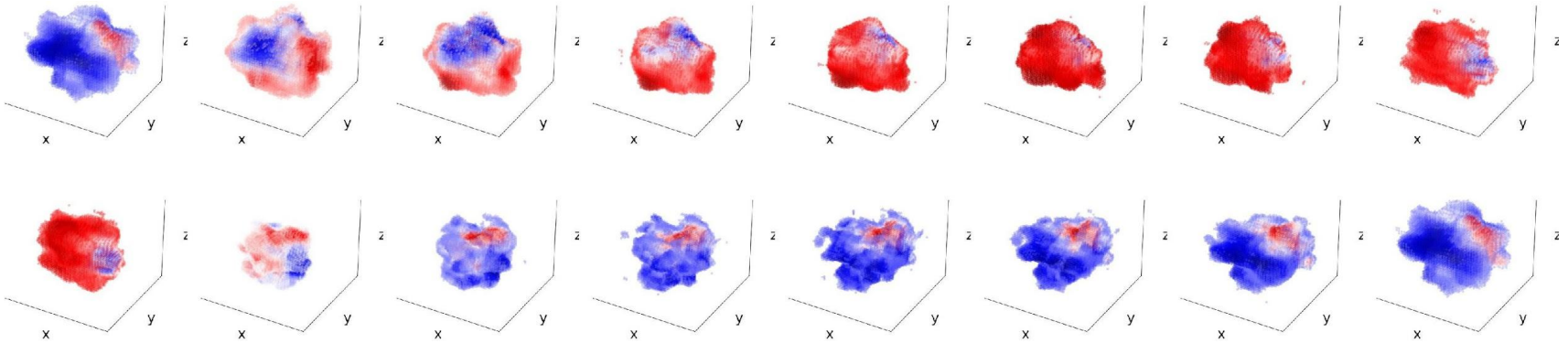

Tru
e

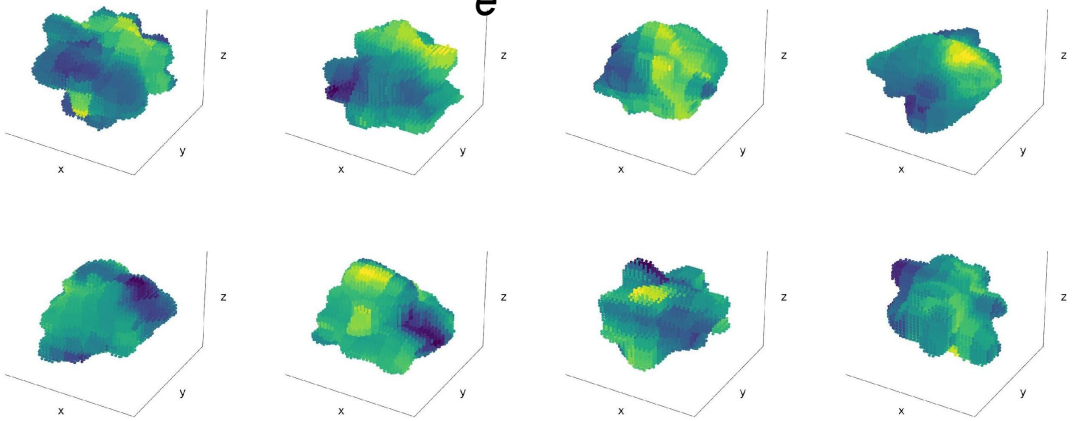

3D CNN
Predictions

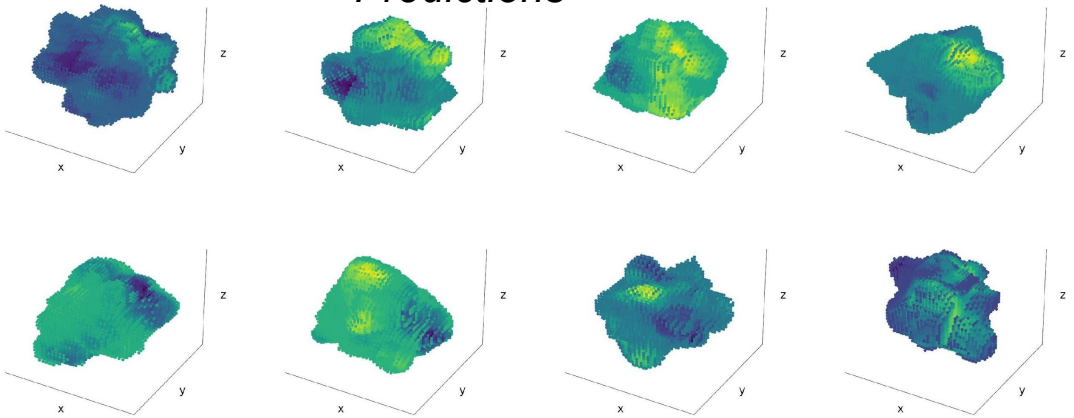

$$I(w)$$

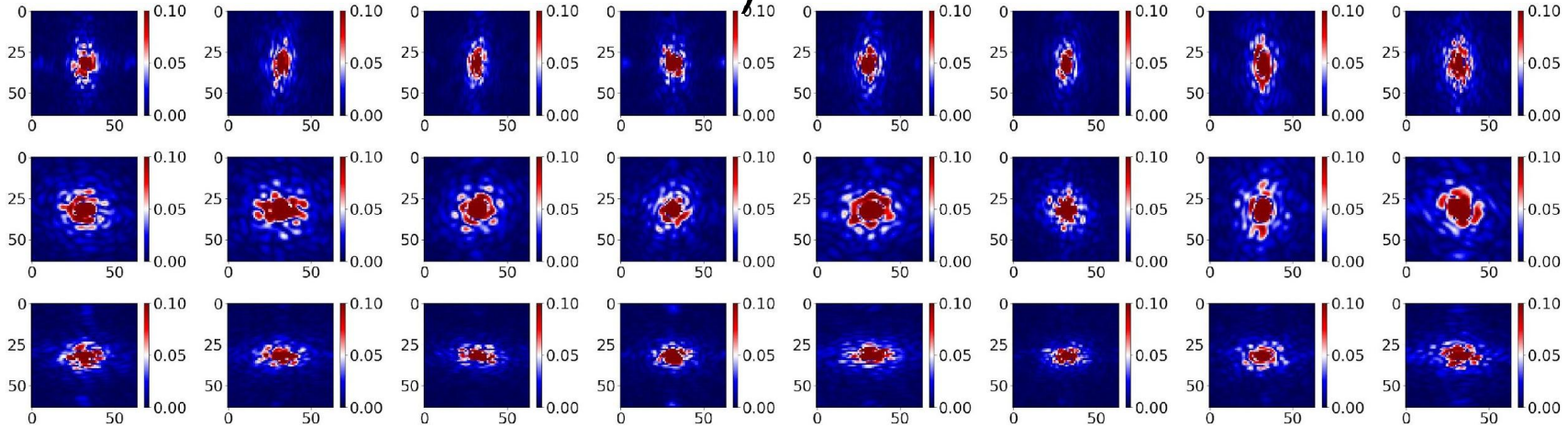

s(**r**)

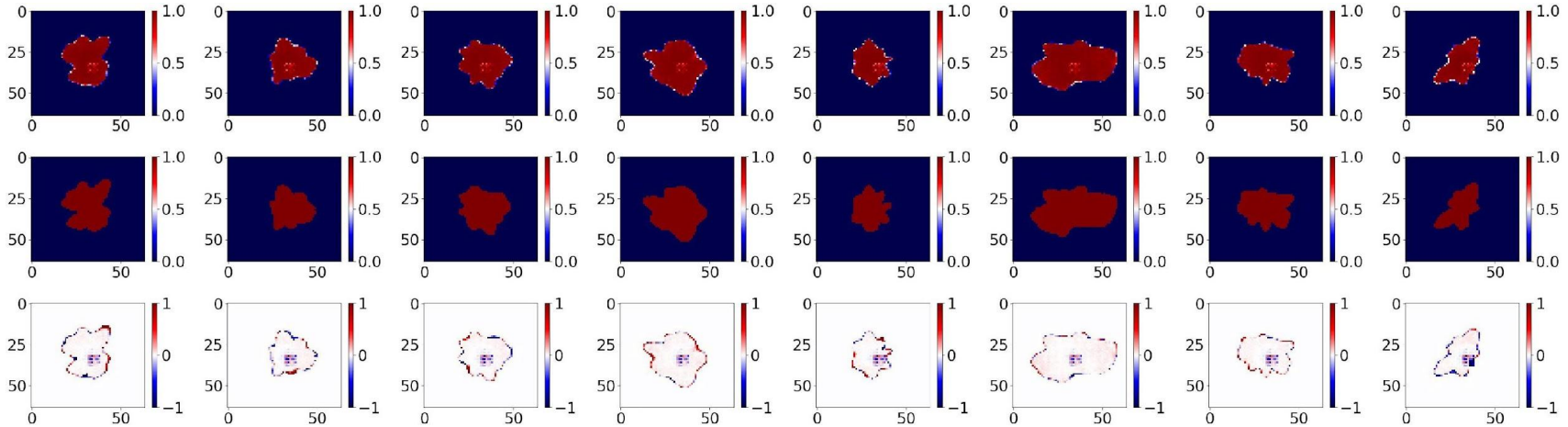

¢(r)